Accepted Manuscript

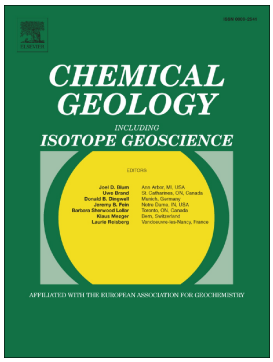

Physical processes occurring in tight gas reservoirs from Western Canadian Sedimentary Basin: Noble gas signature

Magali Pujol, den Boorn, Bernard Bourdon, Matthias Brennwald, Rolf Kipfer

PII: S0009-2541(17)30692-7
DOI: https://doi.org/10.1016/j.chemgeo.2017.12.011
Reference: CHEMGE 18582

To appear in: *Chemical Geology*

Received date: 12 December 2016
Revised date: 4 December 2017
Accepted date: 17 December 2017

Please cite this article as: Magali Pujol, den Boorn, Bernard Bourdon, Matthias Brennwald, Rolf Kipfer , Physical processes occurring in tight gas reservoirs from Western Canadian Sedimentary Basin: Noble gas signature. The address for the corresponding author was captured as affiliation for all authors. Please check if appropriate. Chemge(2017), https://doi.org/10.1016/j.chemgeo.2017.12.011

Physical processes occurring in tight gas reservoirs from Western Canadian Sedimentary Basin: noble gas signature

Magali Pujol [1*], Sander Van den Boorn[2], Bernard Bourdon[3], Matthias Brennwald[4] and Rolf Kipfer[4]

[1] ETH, Institut für Geochemie und Petrologie, Clausiusstrasse 25, 8092 Zürich, Switzerland

*Present day address: Total EP, CSTJF, Avenue Larribau, 64000 Pau, France

[2] Shell Projects and Technology, Kessler Park 1, 2288 GS Rijswijk, Netherlands

[3]Laboratoire de Géologie de Lyon, ENS Lyon, CNRS, and UCBL, Lyon, France

[4]EAWAG, Department of Water Resources and Drinking Water, Dübendorf, Switzerland

(Corresponding Author: magali.pujol@total.com)

Abstract 298 words

Main text 5737 words

Abstract

Noble gases have become a powerful tool to constrain the origin of fluids as well as the rates of fluid migration in sedimentary basins. The aim of this study was to apply these tracers to understand the genesis and the evolution of unconventional gas reservoirs, basin-centered gas reservoirs (also called tight-gas reservoirs). A natural laboratory for this study is the methane-rich gas field in Cretaceous tight sands from the Western Canadian Sedimentary Basin (WCSB). The selection of the WCSB was motivated by an easy access to wells that cover an extensive area from deep to shallow parts of the basin, as well as the relatively well documented geology and hydrology of the area. The elemental noble gas signature (He, Ar, Kr and Xe) of natural gas from 18 wells of the basin shows a mixture between the original low content noble gas signature of the hydrocarbon gas (after its charge into the reservoir) and water (trapped in intergranular volumes (IGV)), which is comparatively rich in noble gases. This difference in relative contents can be used to estimate the geographical position of the contact between the gas reservoir and the shallower IGV water. Furthermore, the 'original' noble gas signature, which is defined as the noble gases generated in the source, later transferred, and mixed with in situ produced noble gases in the reservoir, is mainly composed of radiogenic isotopes (^{40}Ar and ^{4}He). The comparison of $^{4}He/^{40}Ar$ ratios with an average value for potential source rocks and reservoir rocks production ratio (estimated with U, Th and K concentrations) allows us to understand how the gas was transferred from the source rock to the reservoir rock. These results, combined with the geological and hydrological knowledge of the WCSB, affords a new method to better understand the dynamics of unconventional gas reservoirs.

1. Introduction

The noble gases (He-Ne-Ar-Kr and Xe) are chemically inert and their properties vary gradually as a function of their atomic mass. In fact, the solubility of noble gases in water increases from He to Xe whereas it decreases in a gas phase with increasing atomic mass (Weiss, 1970a, 1971a ; Crovetto et al., 1981 ; Smith and Kennedy, 1983 ; Smith, 1985 ; Kharaka and Specht, 1988 ; Harvey, 1998). Noble gases also have numerous isotopes, with some of them being produced by radioactive decay (Wetherill, 1953 ; Steiger and Jäger, 1977), which can be useful to trace the origin of fluids (Pinti and Marty, 1995 ; Kipfer et al., 2002). Due to their inertness and their volatility, noble gases hardly interact with most solid materials. Therefore, terrestrial noble gases tend to accumulate in the atmosphere (except for He), which is the largest noble gas reservoir on Earth (Ozima et Podosek, 2002). Furthermore, the atmosphere has a well defined composition (Basford, 1973) and is in equilibrium with surface waters. As a consequence, any deviation from this natural baseline (atmosphere or surface water) can be easily distinguished. Classically, noble gas composition in natural water is assimilated to Air Saturated Water (ASW) composition which is the noble gas content of water in equilibrium with air at a given temperature (Kipfer et al., 2002). One should note that the isotopic composition of the water (ASW) and air in these conditions are identical.

Over the past decades, numerous studies applied noble gas analyses to sedimentary basins. One of the most common applications is to determine the origin of gas compounds present in the reservoir (Oxburg et al., 1986 ; Ballentine et al., 1991 ; Jenden et al., 1993 ; Ballentine and Burnard, 2002 ; Zhou and Ballentine, 2004 ; Gilfillan et al., 2009 ; Prinzhofer et al., 2010). Also, as they reflect directly the physical processes, noble gases can also be used as a proxy to trace hydrocarbon migration from the source rock to the reservoir rock in sedimentary basins (Prinzhofer and Pernaton, 1997 ; Gilfillan et al., 2009).

The exploitation of unconventional reservoirs such as basin centered gas fields (BCG fields) by petroleum companies has significantly increased over the last decade. These reservoirs represent most of methane reserves in the world and the WCSB would represent 62% of the world reserves (Hiyagon and Kennedy 1992). To illustrate the main differences between Basin Centered Gas (BCG) field and a classical gas field, a simplified cartoon is presented in Figure 1. In the classical model, during gas migration from the source rock to the reservoir rock, gas migrates up through IGV (Intergranular Volume) filled by water. Water and gas are first mixed and are then organized by density (gas phase above water phase). In BCG fields, the porosity is extremely low in the reservoir rocks. During its migration, the gas pushes out main part of the water present in IGV creating a non equilibrated fluid column where the water phase is upper the gas phase (Tobin et al., 2010). This transitional state evolves through time, as the pressure difference decreases and the gas is slowly lost from the reservoir (Yuan et al., 2014 ; Amiri et al., 2015). To evaluate the evolution of such a reservoir, it is thus important to know the amount of gas is still contained in the reservoir and the importance of the water-gas contact zone, equivalent to the volume of gas impacted by water (Burnie et al., 2008).

To accurately build up a basin model, even for an unconventional play, several aspects have to be constrained (Hantschel and Kauerauf, 2009). First, the geological history needs to be known as precisely as possible; this includes how and when the sedimentary basin was formed, the diagenesis of the organic matter, the time of gas cracking, also the type of organic matter responsible for the oil/gas generation. This includes also the evolution of temperature and pressure in the basin, which are important drivers for fluid migration. Second, once the gas is formed, it is important to know the nature and pathways of the gas flow from the source rock (kitchen) to the reservoir(s). If all these parameters are well constrained, it is possible to accurately estimate how much and where the gas is stored in the reservoirs.

Noble gas studies are mainly applicable to the second aspect: the radiogenic noble gas signature of reservoir gas, compared to the source rock composition in U, K and Th (so the calculated production of ^{4}He and ^{40}Ar), can provide insights into the migration process. The non-radiogenic noble gases of reservoir gas presumably come from a contact with an aquifer, so their composition can help determine the geographical limits of reservoir.

In this study, we analysed noble gases in unconventional gas reservoirs in Alberta with the goal of studying the physical properties and processes occurring in the basin, such as the position of the water-gas contact and the gas migration processes in a low porosity medium. Geophysical tools commonly used to determine the extensions of reservoirs or the position of faults can hardly be applied to unconventional reservoirs due to the low contrast of seismic signal between reservoir and cover rocks and also due to the lack of visibility of gas phase in seismic imaging (Meckel and Thomasson, 2008).

2. Basin geology

The geological history of Western Canada Sedimentary Basin has been intensively studied over more than four decades (Hichton (1968), Prather and Mc Court (1968), Masters (1979), Hiyagon and Kennedy (1992), Newson (2004), Webb et al. (2005) Ross and Bustin (2008) and references therein.) due to its petroleum and gas interest. It represents one of the largest natural gas reserves in the world and this natural gas contains more than 80% of methane. Nevertheless, this basin is considered as an unconventional reservoir as the gas reservoirs are different from the classical examples depicted in Figure 1, where an impermeable media overlying a reservoir with high porosity prevents gas escape. The Western Canadian Sedimentary Basin (WCSB) is a broad syncline fold. Its main axis is oriented N-S, on the eastern side of the Rocky Mountains, Alberta. These types of gas fields are called "basin centered gas" because the gas is located in the deepest central part of the syncline fold (and as a consequence there is an updip contact with the overlying aquifer), or "tight gas

reservoirs" due to the low porosity and low permeability of these reservoirs, the consequence of which is that it prevent the water infiltration in its deeper sections (Figure 2, modified from Masters, 1979).

The evolution of the WCSB can be split into two distinct phases (Hiyagon and Kennedy, 1992). The Paleozoic to Jurassic platformal series, dominated by carbonate rocks, was deposited on the stable craton adjacent to the ancient margin of North America. The overlying mid-Jurassic to Paleocene foreland basin series, dominated by clastic rocks, is contemporaneous to the formation of the Canadian Rocky Mountains. Reservoir rocks are mainly composed of Cretaceous siltstones/sandstones strata from the foreland basin. From West to East, the reservoirs are separated into three parts: (i) the disturbed zone, which is geologically complex represented by the central part of the syncline fold, under the Rocky Mountains, (ii) the highly pressurized zone (Intergranular Volume Pressure, P_{IGV} >> hydrostatic Pressure, $P_{hydrostatic}$), where most of the gas is stored and, (iii) the underpressurized zone ($P_{IGV} \leq P_{hydrostatic}$) which is close to the water-gas contact in the northeast. The source rocks have not been clearly identified and they could originate both from oceanic organic matter (Jurassic) or continentally-derived organic matter (Cretaceous). These source rocks mainly generated CH_4-rich gas (more than 80%), without any oil production (primary gas generation).

3. Sampling strategy

In order to evaluate the importance of gas-water interaction, sampled wells covered from the highly pressurized zone of the basin up to the underpressurized zone. The main issue was that each well could cross several reservoirs on the same vertical line. None of reservoirs is actually continuous throughout the basin; most reservoirs have the shapes of lenses (Figure 2) that are not necessarily in contact with each other. Thus, the gas sampled from the well represent a mixture between all reservoirs on the same vertical line (up to 8, as shown in

Figure 2), in which case the gas is said to be "commingled". The geographic location of the sampled wells is shown in Figure 3.

Source rock samples were taken from drill core of the high pressurized zone of the basin, stored in the core laboratory of Calgary. These were selected from different depths as an attempt to determine which source rock(s) is (are) responsible for gas production. Reservoir rock samples were also chosen. Noble gas signature, especially radiogenic noble gases, is supposed to reflect the source rock initial noble gas signature. Nevertheless, as reservoir rock volumes are more important than source rock volume, by a factor of about 20, and even if the radiogenic in situ production within reservoir rock is limited (poor K, Th and U content compared to source rock content), it is expected that the source rock noble gas signature is diluted and the "initial" gas measured in samples is actually a mixing between source and reservoir in situ produced noble gases.

4. Sampling and analytical methods

The CH_4-rich natural gas samples were collected by field operators in ~500 cc stainless steel gas cylinders sealed at each end with bellow valves. From each individual well, samples were taken using two different sampling methods. In both cases, the cylinders, pre-evacuated by AGAT Company (Edmonton, Canada) to a pressure of 17mm Hg (i.e. 22.7 mbar), were attached to the sampling port located after the separator (which separates the gas from liquid components) on the well site. Once attached, one of the cylinders was filled with gas directly without purging, whereas for the other method, the cylinder was purged for 15 seconds with natural gas before taking the sample. It appeared all samples that were not purged were too polluted by air to be interpreted and this study reports only results from the purged samples (Gilfillan et al., 2008 ; Gyore et al., 2015 ; Barry et al., 2016). All gas samples were analyzed for noble gas composition at ETH Zurich (Switzerland) using the same method as that described by Beyerle et al. (2000) which was designed for noble gas

analyses in water samples. An additional purification step was included in the extraction line specifically for handling natural gas. As all samples contained >80% of CH_4, the first step was to remove most of the hydrocarbons before introducing the sample into the rest of the purification line. This was achieved by fluxing the gas over two chemical traps (getters). These getters consisted of titanium sponges with a very high adsorption capacity and surface area. They acted to break down molecules containing hydrogen (e.g. hydrocarbons, and H_2O), which is most efficient at high temperature, the best efficiency being reached between 600 and 700°C. The getters were operated one after the other for 10 minutes at high temperature (650±50°C) and 10 minutes at room temperature. At high temperatures, hydrogen radicals are released in the line, whereas the other molecules remained adsorbed on the Ti sponge. At room temperature the reactions are reversed and hydrogen radicals were adsorbed whereas the remaining molecules were released. The purification process is optimized by allowing the connection between the two getters to be open when the second one is at high temperature, such that that the released H radicals were trapped by the first getter which was at room temperature. These getters also trap CO_2, O_2 and N_2 which are common contaminants in many terrestrial gas samples.

Source and reservoir rocks were ground to powder and sent to SARM (Service d'Analyse de Roches et Minéraux, CRPG, Nancy, France). The chemical composition of these rocks was measured by ICP-AES for major elements and ICP-MS for trace elements. Table 1 reports U, Th and K compositions which are producing noble gases: ^{4}He is produced by decay of U and Th while ^{40}Ar is produced by decay of ^{40}K.

5. Results

All the noble gas results are reported in Table 2. Ne isotopes were measured but are not reported because ^{20}Ne and ^{22}Ne contents were about 2 times the blank value. Except for ^{4}He and ^{40}Ar, all noble gas contents were very low in the gas phase: Xe and Kr for example are

up to 1000 and 100 times respectively less concentrated than in the ASW composition. Nevertheless, as a typical blank represents less than 1% (10% for Xe isotopes,) of the content measured in a sample, the results reported in Table 2 are corrected for blanks.

As shown in Table 1, the four reservoir rocks show rather homogeneous concentrations in U, Th and K (within a factor of 2). These reservoir rocks should be representative of the main reservoir rocks composition. In contrast, the compositional variability of the source rocks is quite large (up to a factor of 100). However, since the most productive source rock, if it really exists, could not be identified, we used instead the average of these compositions.

6. Estimation of the "initial" gas signature in the reservoir

The noble gas analyses were used to constrain the state and evolution of the natural gas from the WCSB. To achieve this goal, the noble gas signature of the gas contained in the reservoirs (without any modification due to migration or contact with water) has first to be characterized. The gas was generated in the source rock, then migrated to the reservoir rock and noble gases from the source rock were diluted by noble gases initially present in the reservoir, we call this signature "initial noble gas signature". Once this signature is determined, it is possible to distinguish it from any secondary modification, and this, in turn, can help understand the origin of these modifications.

As the gas sampled from each well is commingled see Figure 1), the noble gas signature recorded in our samples must also reflect the mixture between different reservoirs. The gas found in each reservoir could also have been derived from different underlying source rocks. Thus, due to this mixing process, it is difficult to extract a source signature specific to a given source rock. Nevertheless, a common trend is obvious in a plot of Kr versus Xe contents (Figure 4 Left panel). There is a clear mixing line between a component depleted in heavy noble gases and a component identified as representing the formation water. The component depleted in heavy noble gases by a factor of 100 to 1’000 times relative to ASW must

represent the signature of the reservoir gas that has been preserved despite these low contents. If we combine the quasi-absence of heavy primordial noble gas with the high ^{4}He content and the very low $^{3}He/^{4}He$ ratios (Figure 4 Right panel), one infers that the noble gas signature is highly radiogenic. This fact can be explained by an early loss of initial atmospheric noble gas from the future source rock (and maybe also from the future reservoir rocks) during diagenesis (due to their loss with increasing pressure and temperature). The loss of noble gas in source rocks (and/or reservoir rocks) is compensated by enrichment in radiogenic noble gas due to in situ production by radioactive decay of U, Th and K (producing mainly ^{4}He and ^{40}Ar). Following this early noble gas loss, during the gas charge in the reservoir, the water is pushed out of the reservoir, and only residual water and in situ produced noble gas are mixed with the charged natural gas. The initial signature of the noble gases measured in reservoirs is purely radiogenic (i.e. it can be attributed to the effect of radioactive decay), and with this signature it is possible to discriminate the subsequent effect of kinetic mass fractionation or mixing with water.

7. Discussion

As described before, noble gas can be used to examine the mode of gas transport by comparing the theoretical radiogenic noble gas signature produced in source and reservoir rocks. In addition, the non-radiogenic noble gases of the reservoir are highly sensitive to interaction with water, such that their composition can help determine the geographical position of the gas/aquifer interface.

7.1. Non radiogenic noble gas signature: lateral extension of the reservoirs

An important target of this study was to understand the contact between the gas reservoirs and the aquifers. Theoretically, as the gas in the reservoirs has an almost pure radiogenic

noble gas signature, when the analysed gas is sampled closer to the water contact zone, the fraction of noble gases coming from the updip aquifer such as ^{36}Ar, Kr, or Xe should increase. To investigate this, ^{36}Ar contents were plotted as a function of depth of a reservoir formation present in all wells. As shown in Figure 2, the depth of this reservoir increases from the NE to the SW. In Figure 5, a trend from the shallower part of the basin, enriched in ^{36}Ar compared with the deeper part which has low ^{36}Ar content can be observed. One should note that four wells represent exceptions to this trend, as they are enriched in ^{36}Ar while being located in the deeper part of the basin, this fact will be discussed in section 8.

In figure 5, the ^{36}Ar content represents a proxy for the exchange of gas in the reservoir with aquifer. Indeed, when the water is in contact with the gas for the first time, most of ^{36}Ar from the water phase is transferred into the gas phase, as the CH_4/water partition coefficient for noble gases is much higher than 1 and decreases from light to heavy noble gases (Zartman et al. 1961). However, if the same residual water, which has lost its noble gases by interaction with CH_4, is one more time in contact with gas, this gas will not be enriched in ^{36}Ar, but will have a noble gas signature characterized by a larger abundance of heavy noble gas than light ones and an overall low noble gas contents (noble gas poor water (NGP water)). Thus, to fully highlight the effect of interaction with water on the noble gas composition, the evolution line of ^{136}Xe/^{36}Ar and ^{84}Kr/^{36}Ar ratios with successive contacts with water are illustrated in Figure 6. When plotting our data on the same diagram (Figure 7, Left panel), it is obvious that the composition of five wells which were not enriched in ^{36}Ar followed the water “distillation trend”, which means that these wells were in contact with water that has interacted repeatedly with gas. These wells with NGP water signature were represented on a map in Figure 7, Right panel. Focussing on the north-eastern region of the field area, which is the shallowest and underpressurized part of the basin close to the water-gas contact, noble gas composition evolves gradually from the central part of the basin (with no noble gas water signature in the gas) through the northeast (NGP water signature in the gas) until an estimated position of the aquifer (not distillated water noble gas composition in

the gas). The two closest wells from the water-gas contact show a strong influence of a water signature (high ^{36}Ar), whereas the three wells located to the southwest of the water-influenced wells shows an influence of NGP water and then the two wells farther in the southwest direction show no influence of water. Combined with the general SW-NE direction of gas migration (Jones et al. (1985), Majorowicz et al. (2013)), this indicates that the gas was first formed in the deeper part of the basin, migrated upwards along a northeast direction, thereby pushing the water along a NW-SE trending contact.

In the southwest region of the basin which corresponds to the deepest reservoirs, the situation is obviously more complex. This can be explained by the complexity of water circulation in this area due to the presence of a faulting system (Masters, 1979). Indeed, closer to the syncline axe, there are different directions of water flows (Bacchu et al., 1999). In conclusion, there are updip contacts both in the northwest, and in the north. Concerning the observed water influence in the central part of the basin (wells #8 and #18), a downdip contact with an aquifer is suspected. Indeed, as the fluid column in BCG reservoirs is unstable, it tends to reorganize by densities (gas phase above water phase) (Weides et al., 2014 ; Tobin et al., 2010 ; Majorowicz et al., 1999).

7.2 Radiogenic noble gases signature

As explained in section 6, the noble gas composition of the generated gas in the reservoir is almost purely radiogenic. Thus, the study of the radiogenic noble gas composition provides information on what happened to the gas before any mixing process with water. One can infer the gas migration process (diffusive versus Darcy flow) and the apparent age of the gas.

First, it is possible to determine how the gas is transferred from the source rock to the reservoir rock in the low porosity / low permeability system. An estimation of the Peclet number (Pe) in the sedimentary basin is needed to determine if the mass transfer is preferentially diffusive or advective (Darcy flow). It is not possible to calculate Pe precisely

due to variations in the permeability and bad estimations of characteristic lengthscale. Nevertheless, Bacchu et al. (1993) estimated a value of Pe<10 for methane transfer, which means that the preferential mode of mass transfer in the basin is molecular diffusion, as expected in tight environment. With the noble gas signature it is possible to distinguish for each well between an advective gas transport (i.e. Darcy flow corresponding in fact to the absence of differential transport between noble gas species) and a diffusive transport where the signature was subjected to kinetic mass fractionation.

For this purpose, the amounts of $^{40}Ar^*$ were calculated and plotted in Figure 8, Left panel, showing ^{4}He versus $^{40}Ar^*$ compositions for each well gas. This was then compared with the predicted trend for an in situ production in the source and in the reservoir itself, based on their respective averages of U, Th and K production ratios. Three different cases are possible. First, if $^{4}He/^{40}Ar^*$ ratios are compatible with ratios typical for source rocks or reservoir rocks, or a mixture of both, it means that the initial signature was preserved and that the transport was mainly advective during the charge. Second, if ^{4}He is enriched relative to $^{40}Ar^*$, the initial signature was not preserved and the effect of diffusion depleted the heavy gases (here Ar) compared to the lighter ones (He). Last, $^{40}Ar^*$ can be enriched relative to ^{4}He, this latter case meaning that the lightest isotopes were probably lost by leakage of the reservoir.

In Figure 8, Left panel, three groups of wells can be identified, corresponding to the three cases described above: the first group is characterized by a high $^{4}He/^{40}Ar$ ratio compared with the radiogenic production ratios estimated in the source and the reservoir, the second group fits with the radiogenic “production line” with $^{40}Ar^*/^{4}He$ ratios ranging between the source and reservoir production ratio and the last group composed of two wells shows an apparent excess of radiogenic $^{40}Ar^*$.

The radiogenic noble gas compositions from the first group enriched in ^{4}He can be explained by a diffusive transport from the source rock to the reservoir rock. Considering the low Péclet

number, it is not surprising to have a highly diffusive transport where the lighter elements migrate preferentially to the reservoir rock. Furthermore, the observation of a diffusive transport widely spread in the field proves that the source rock is clearly distinct from the reservoir rock (no in situ CH_4 generation).

The signature of the second group can be explained by advective transport. The data lie on a well defined trend intermediate between the average production ratio of source and reservoir rocks. Considering the numerous stacked reservoirs and the numerous potential source rocks in the basin, it is surprising to observed such an homogeneous trend. It can be taken as evidence for mixing of the gas from different reservoir rocks and/or of production by a single source rock formation. The wells which have a low content in both ^{4}He and ^{40}Ar can also be explained by a diffusive transport combined with a loss of $^{4}He^{*}$. It should be noted in this case that the loss in He has to match exactly the enrichment inherited from diffusion. This could seem as fortuitous, hence this interpretation is considered as ad-hoc.

The third group composition depleted in ^{4}He is composed of two wells from the northeastern part of the basin. This can be due to the loss of lighter elements from the reservoir. Nevertheless, it is important to point out that for both wells (Figure 8, Right panel), the $^{40}Ar/^{36}Ar$ ratio is just slightly above the atmospheric ratio and that the only reason for the high content of $^{40}Ar^{*}$ is the high content of total Ar (100 times more than the average composition of wells). Thus, these wells did not lose He, but were enriched in Ar by the contact with an aquifer which would have brought at the same time important amounts of ^{36}Ar and ^{40}Ar.. Moreover, their geographic position in the northeastern part of the basin and the study of non-radiogenic noble gas (section 6.2) confirm a contact with an updip aquifer, presumably far from the atmospheric recharge area because of the slight enrichment in $^{40}Ar^{*}$. This slight enrichment is due to aquifer circulation through rocks containing K, after the time of atmospheric recharge. .

Considering the geographical distribution of noble gas compositions (Figure 8, Right panel), a trend can be observed from the NE to the SW. In the lower pressured part of the basin (Meckel et Thomasson, 2008), well signatures are more and more depleted in ^{4}He for a similar $^{40}Ar^{*}$ content. In the higher pressured deep basin, the charging system is dominantly advective in the NW area, and diffusive (to highly diffusive with no excess in $^{40}Ar^{*}$) in the rest to this area.

8. General implications

First, the noble gas signature of the natural gas derived from the source rocks was shown to be purely radiogenic. This radiogenic signature bears some meaning about the evolution of the gas prior to contact with water. The diagram ^{4}He as function of $^{40}Ar^{*}$ (Figure 8, Left panel) shows all wells have roughly the same ^{4}He content around 5×10^{-5} ccSTP/cc, except for three wells that are enriched in ^{4}He up to a factor of 4. Using the average ^{4}He content, it is possible estimate the time necessary to accumulate the observed ^{4}He based on the measured U and Th contents in cores. A few assumptions needs to be made to estimate an apparent ^{4}He age: (i) all ^{4}He is sited in intergranular volume with a reservoir porosity of 5%, (ii) fluid pressure is about 5×10^{7} Pa (hydrostatic pressure at 5000 m depth, corresponding to 3000m deep gas which had a 2000m uplift) and gas temperature is about 363 K, (iii) gas consists of pure methane and, (iiii) reservoir rock density is about 2800 kg/m^{3}. Given all these assumptions, the accumulated ^{4}He can be estimated following the equation (Craig and Lupton, 1976 ; Battani et al., 2011):

$$(^{4}He) = (3.115 \times 10^{6} + 1.272 \times 10^{5})\,[U] + 7.710 \times 10^{5}\,[Th].$$

Where (^{4}He) is the He production rate in $atoms.g^{-1}.y^{-1}$, and [U] and [Th] are respectively uranium and thorium concentrations in $10^{-6}.mol.g^{-1}$

First, as the density of CH_4 changes with pressure due to its non negligible compressibility factor, and has to be estimated in the P and T conditions of the reservoir:

$\rho(CH_4) = \rho_0 \times \frac{P}{P_0}$ with ρ_0 the density of CH_4 at a pressure P_0 of 1atm and 0°C,

Using the ideal gas law for He, with a deviation factor of 1.06 (representing an ideality deviation, calculated under standard temperature and pressure), one obtains 3.63 x 10^{-3} mol of ^{4}He per kg of fluid. To convert it into mol per kg of rock, the following equation can be used:

$$M_f / M_{tot} = \frac{\rho_f \phi}{\rho_f \phi + \rho_r (1-\phi)}$$

with M_f and M_{tot} being the mass of fluid and total mass (fluid + rock), respectively, ρ_f and ρ_r being the density of the fluid and of the rock and Φ the porosity, respectively.

Applying this equation, the concentration of ^{4}He is 3.75 x 10^{-3} mol /kg, which is equivalent to an approximate ^{4}He age of 578 million years. This age is clearly higher than the age of the rock, which implies that ^{4}He amount is not only due to the production in the source rock. Nevertheless, this result is realistic as the gas produced is charged in the reservoir rock mainly by diffusion. The estimated source rock is located between 0 and 500 m under the estimated reservoir rock. As a consequence, the gas has to cross a large amount of rock which contains some U, K and Th and which also produces some ^{4}He that can be collected by the migrating natural gas (open system). Our suggestion is that this ^{4}He produced in the thickness between the source rock and the reservoir rock above is carried in the gas stream during the gas migration to the reservoir (Figure 9). This hypothesis can be illustrated by the 3 wells enriched in ^{4}He (wells #1, #7 and #8), which, due to their geographical position, traveled the longest way from the kitchen (producing source rock in the central part of the basin) to the limit of the reservoir close to the water contact. Wells #6, #2 and #18 do not

show ^{4}He excesses presumably due to an exchange of ^{4}He with the water phase as explained in section 7.2.

The wells located in the NW (wells #16, #14, #10, #17, and #5) are characterized by a similar radiogenic noble gas signature, even though many reservoirs and possible source rocks are involved, this indicate that there were a mixing within the reservoir possibly through a fault system.

To summarize, the wells in the field can be separated in three different geographical areas according to the behaviour of their noble gases (Figure 10): the NE area, the NW area and the S.

First, on the NE area, both radiogenic and non radiogenic noble gas signatures show a NE-SW trend. The main gas flow is estimated to be from the SW to the NE (Bacchu et al., 1999), which correlates with our observations, showing an increasing influence of water towards the NE. The gas was first generated in the central part of the basin and is flowing upward, pushing the water-gas interface towards the NE. The non-radiogenic noble gas composition of this first generated gas clearly shows a water influence. Moreover, there is a correlation between the type of transport (from radiogenic noble gases) and the degree of interaction with water (from non radiogenic noble gases) (Figure 10). In the NE part, a direct influence of water is associated with a preferential loss of ^{4}He, compatible with noble gases exchange with water phase poor in ^{4}He. This progressive loss of ^{4}He disappears through the south west, combined with the decrease of water influence, which confirms the gas migration direction and the geographical position of the water/gas contact.

In the deeper part of the basin, there is no clear trend as in the north eastern part, but there is still a correlation between the type of transport and the degree of interaction with water. Focussing on the NW area, an interaction with water (normal or noble gas poor water) is linked to an advective transport. This can be explained by water flow along a fault system (hydraulic fracturation), and not necessarily by any water/gas contact.

In the southern part of the basin, well #18 (and probably also well #8) are sitting on a downward dipping aquifer in Lower Devonian terranes (Weides et al., 2014 ; Majorowicz et al., 1999). It is possible that the measured water influence is not a direct gas water contact but results from the diffusion/percolation effect of noble gases from this aquifer into the reservoirs (Burnie et al., 2008).

9. Conclusions

In conclusion, noble gases are a useful tool to understand the physical processes related to the evolution of unconventional gas reservoirs. This noble gas study in the intensive drilled area could afford useful information about how some natural gas can fill a tight reservoir (fault system vs. diffusion). Radiogenic noble gas, reflecting the initial signature of the source rock, showed the main transfer process in this basin is diffusion, proved by the relative enrichment in ^{4}He compared to $^{40}Ar^{*}$. Some advective transfers (Darcy flow) were also brought out and appeared to be systematically linked to the presence of water. Thus the interpreted gas flow fits with the regional water flow (Weides et al., 2014 and references therein). This can be explained by a hydraulic fracturation created by the water flow in the basin. It can be interested to confirm this hypothesis with hydrocarbon relative concentrations. If methane / ethane concentrations ratios, for instance, are higher in "diffusive transfer zones" than in "advective transfer zones", then it can prove that noble gas compositions are a good tool to spotlight hydraulic fracturation zones even if fractures are presently sealed.

After the gas charge into the reservoir, noble signature can be modified by an eventual leakage or by a contact with an aquifer. As noble gas solubility is much higher in gas phase than in water phase (Ballentine and Burnard 2002) and as noble gas initial content is in favour of water, unidirectional gas flux from water phase to gas phase can be approximated. Then noble gas water signature is superimposed on noble gas signature from gas phase which explains why the initial signature is not lost. In this case study, gas was sampled

randomly from different parts of the basin from the deepest central part of the basin up to close to gas basin borders. This kind of sampling showed that the noble gas water signature are situated close to basin borders, and even more that the closer to the aquifer the sampled gas is, the more concentrated the noble gas water signature is. In conclusion, due to their inertness, noble gases isotopic and elemental compositions appear to be a useful tool to better constrain and understand physical transfer and exchanges in unconventional reservoirs. Nevertheless, like most of other methods, it becomes powerful when it is integrated with other geological and fluids understanding to build an accurate basin model.

Acknowledgements

We would like to thank first Larry Paulson, Shell Canada Upstream, Edson Field Office, for his great help on the field**,** his constant good mood and all our cultural differences exchanges. Then, Philip Benham, Shell Canada Energy, spend lots of time explaining us the basin sedimentology. Finally, Volker Dickmann, Olaf Podlaha and all the organic geochemistry team, Shell Projects and Technology, Rijswijk, thank you for all the fruitfull exchanges during these 2 years of work, they showed how much the communication between different scientific communities helps the global understanding.

References

Amiri M., Zahedi G. And Yunan M.H. (2015) Reducing predictive uncertainty in log-derived water saturation models in giant tight shaly sandstones – A case study from Mesaverde tight gas reservoir. J. Nat. Gas Sci. & Engin., vol. 23, pp 380-386.

Bachu S., Underschultz J. R., Hichton B., and Cotterill D. (1993) Regional-scale sudsurface hydrogeology in northeast Alberta. Edmonton: AGS/ARC, Bull. 61, 44 p.

Ballentine C.J., O'Nions R.K., Oxburgh E.R., Horvath F. and Deak J. (1991) Rare gas constraints on hydrocarbon accumulation, crustal degassing and groundwater flow in the Pannonian Basin. Earth and Planet. Sci. Lett., vol. 105, pp 229-246

Ballentine C.J. and Burnard P.G. (2002) Production, release and transport of noble gases in the continental crust. Rev. Mineral. Geochem., vol. 47, pp 481-538.

Barry P. H., Lawson M., Meurer W. P., Warr O., Mabry J.C., Byrne D.J., and Ballentine C.J. (2016) Noble gases solubility models of hydrocarbon charge mechanism in the Sleipner Vest gas field. GCA, vol. 194, pp 291-309.

Basford J.R., Dragon J.C., Pepin R.O., Coscio Jr. M.R. and Murthy V.R. (1973) Krypton and xenon in lunar fines. In Proc. Lunar Sci. Conf., vol. 4, pp 1915-1955.

Battani A., Smith T., Robinet J.-C., Brulhet J., Lavielle B., and Coelho D. (2011) Contribution of logging tools to understanding helium porewater data across the Mesozoic sequence of the East of the Paris Basin, GCA, vol. 75, pp 7566-7584.

Beyerle U., Aeschbach-Hertig W., Imboden D.M., Baur H., Graf T., and Kipfer R. (2000) A mass spectrometric system fort he analysis of noble gases and tritium from water samples. Environ. Sci. Technol., vol. 34, pp 2042-2050.

Burnie Sr S.W., Maini B., Palmer B.R. and Rakhit K. (2008) Experimental and empirical observations supporting a capillary model involving gas generation, migration, and seal

leakage for the origin and occurrence of regional gasifers. In Understanding, Exploring, and Developping Tight-gas Sands, AAPG Hedberg Series, vol. 3, pp 29-48.

Craig H., and Lupton J.E. (1976) Primordial neon, helium and hydrogen in oceanic basalts, Earth Planet. Sci. Lett., vol. 31, pp 369-385.

Crovetto R., Fernandez-Prini R. and Japas M.L. (1981) Solubility of inert gass and methane in H2O and D2O in the temperature range of 300 to 600 K. J. Chem. Phys., vol. 76, pp 1077-1086.

Gilfillan S.M.W., Sherwood-Lollar B., Holland G., Blagburn D., Stevens S., Schoell M., Cassidy M., Ding Z., Zhou Z., Lacrampe-Couloume and Ballentine C.J. (2009) Solubility trapping in formation water as dominant CO_2 sink in natural gas fields. Nature, vol. 458, pp 614-618.

Gilfillan S. M. W., Ballentine C. J., Holland G., Blagburn D., Sherwood Lollar B., Stevens S., Schoell M., and Cassidy M. (2008) The noble gas geochemistry of natural CO_2 gas reservoirs from the Colorado Plateau and Rocky Mountain provinces, USA. GCA, vol. 72, pp 1174-1198.

Györe D., Stuart F.M., Gilfillan S.M.V., and Waldron S. (2015) Tracing injected CO_2 in the Cranfield enhanced oil recovery field (MS, USA) using He, Ne and Ar isotopes. International Journal of

Harvey A.H. (1998) Application of near-critical dilute-solution thermodynamics. Ind. Eng. Chem. Res., vol. 37-8, pp 415-424.

Hantschel T., and Kauerauf A.I. (2009) Fundamentals of basin and petroleum systems modelling. Eds Springer.

Hichton B. (1968) Geochemistry of natural gas in Western Canada. In Natural Gases of North America (ed. B.W. Beebe and B.F. Curtis), Amer. Assoc. Petrol. Geol. Mem., vol.), pp 1995-2025.

Hiyagon H. and Kennedy B.M. (1992) Noble gases in natural gas of Alberta, Canada. Geochim. Cosmochim. Acta, vol.56, pp 1569-1589.

Jenden P.D., Hilton D.R., Kaplan I.R. and Craig H.(1993) Abiogenic hydrocarbons and mantle helium in oil and gas fields. In “The future of natural gas”, D.G. Howell, ed. U.S. Geological Survey Professional paper n°1570, pp 31-56.

Jones F., Lam H.L. and Majorowicz J. (1985) Temperature distributions at the Paleozoic and Precambrian surfaces and their implications for geothermal energy recovery in Alberta. Can. J. Earth Sci., vol. 22, pp 1774-1780

Kharaka Y.K. and Specht D.J. (1988) The solubility of nable gases in crude oil at 25-100 °C. Appl. Geochem., vol. 3, pp 137-144.

Kipfer R., Aeschbach-Hertig W., Peeters F. and Stute M. (2002) Noble gas in lakes and groundwaters. Rev. Mineral. Geochem., vol. 47, pp 615-700.

Lee J.-Y., Marti K., Severinhaus J.P., Kawamura K., Yoo H.-S., Lee J.B., Kim J.S. (2006) A redetermination of the isotopic abundances of atmospheric Ar. Geochem. Cosmochem. Acta, vol. 70, pp 4507-4512.

Majorowicz J., Garven G., Jessop A. And Jessop C. (1999) Present heat flow along a profile across the Western Canadian Sedimentary Basin: the extent of hydrodynamics influence. Geothermics in Basin Analysis, Springer: Heidelberg, Germany, pp 61-79.

Majorowicz J., Unsworth M., Chacko T., Gray A., Heaman L., Potter D. and Schmitt D. (2013) Geothermal energy as a source of heat for oil sand processing in northern Alberta, Canada. Heavy oil/bitumen Petreloum Systems in Alberta and beyond, Hein, Leckie, Suter and Larter Eds, AAPG, vol. 64, pp 725-746.

Masters J.A. (1979) Deep Basin gas trap, Western Canada. Am. Assoc. Petrol. Geol. Bull., vol. 63, pp 152-181.

Meckel L.D. and Thomasson M.R. (2008) Pervasive tight-gas sandstone reservoirs : An overview. In Understanding, Exploring, and Developing Tight-gas Sands, AAPG Hedberg Series, vol. 3, pp 13-27.Oxburg E.R, O'Nions R.K. and Hill R.I. (1986) Helium isotopes in sedimentary basins. Nature, vol. 324-18, pp 632-635.

Newson A. (2004) The foothills of Western Canada, a fold and thrust belt natural gas play. Adapted from "extended abstract" for presentation at the AAPG Annual Meeting, Salt Lake City, Utah.

Pinti D.L. and Marty B. (1995) Noble gases in crude oils from the Paris Basin, France: implications for the origin of fluids and constraints on oil-water-gas interactions. Geochim. Cosmochim. Acta, vol. 59, pp 3389-3404.

Prather R.W. and McCourt G.B. (1968) Geology of gas accumulations in paleozoic rocks of Alberta plains. In Natural Gases of North America (ed. B.W. Beebe and B.F. Curtis), AAPG Mem., vol. 9, pp 1238-1284.

Prinzhofer A. and Pernaton E. (1997) Isotopically light methane in natural gases: bacterial imprint or segregative migration? Chem. Geol., vol. 142, pp 193-200.

Prinzhofer A., Vaz Dos Santos Neto E. and Battani A. (2010) Coupled use of carbon isotopes and noble gas isotopes in Potiguar Basin (Brazil): fluid migration and mantle influence. Marine and Petroleum Geol., vol. 27, pp 1273-1284.

Ross D.J.K. and Bustin R.M. (2008) Characterizing the shale gas resource potential of Devonian-Mississipian strata in the Western Canadian Sedimentary Basin: application of an integrated formation. AAPG Bull., vol. 92 (1), pp 87-125.

Smith S.P. (1985) Noble gas solubility at high temperatures. EOS, Trans. Am. Geophys. Union, vol. 66, pp 397.

Smith S.P. and Kennedy B.M. (1983) The solubility of noble gas in water and NaCl brine. Geochim. Cosmochim. Acta, vol. 47, pp 503-515.

Steiger R.H. and Jäger E. (1977) Subcommission on geochronology: convention on the use of decay constants in go- and cosmochronology. Earth Planet. Sci. Lett., vol. 36, pp 359-362.

Tobin R.C., McClain T., Lieber R.B., Ozkan A., Banfield L.A., Marchand A.M. and McRae L.E. (2010) Reservoir quality modelin of tight gas sands in Wamsutter field: integration of diagenesis, petroleum systems, and production data. AAPG Bull., vol. 94(8), pp 1229-1266.

Webb A.C., Schroder-Adams C.J. and Pedersen P.K. (2005) Regional subsurface correlations of Albian Sequences Noth of the Peace River in NE British Colombian: northward extent of sandstones of the Falher and Notikewin members along the eastern flank of the foredeep. Bull. Canadian Petrol. Geol., vol. 53(2), pp 165-188.

Weides S., Moeck I., Majorowicz J., Grobe M. (2014) The cambrian basal sandstone unit in Cantral Alberta – An investigation of temperature distribution, petrography and hydraulic and geomechanical properties of a deep saline aquifer. Can. J. Earth Sci., vol. 51(8), pp 783-796.

Weiss R.F. (1970) The solubility of nitrogen, oxygen and argon in water band seawater. Deep-Sea Res., vol. 17, pp 721-735

Weiss R.F. (1971) Solubility of helium and neon in water and seawater. J. Chem. Eng. Data, vol. 23, pp 69-72.

Wetherill G.W. (1953) Spontaneous fission yields from uranium and thorium. Phys. Rev., vol. 96, pp 907-912.

Yuan L., Sima L. And Wu S. (2014) Models for saturation of the tight gas sandstone reservoir. Petrol. Sci. Tech., vol. 32 (23), pp 2777-2785.

Zhou Z. and Ballentine C.J. (2005) 4He dating of groundwater associated with hydrocarbon reservoirs. Chem. Geol., vol. 226, pp 309-327.

Table captions

Table 1: Chemical composition of source rocks and reservoir rock formations from the Cretaceous Mannville Group. The analyses were made at SARM (Service d'analyses de roches et matériaux, CRPG, Nancy, France).

Table 2: Noble gas composition for gas samples from sampled gas wells. Air composition is from Basfod et al. (1973) except for $^{40}Ar/^{36}Ar$ ratio which was recalculated by Lee et al. (2006). ASW composition equilibrated with 10°C fresh water is from Kipfer et al. (2002).

Table 1: Chemical composition of source rocks and reservoir rocks

Samples	Th ($\times 10^{-9}$ mol/g)	U ($\times 10^{-9}$ mol/g)	K ($\times 10^{-5}$ mol/g)
Source Rock Obed	8.54	4.32	1.06
Source Rock Obed	46.9	26.6	35.4
Source Rock Obed	37.4	15.3	35.2
Source Rock Obed	28.6	17.1	12.5
Source Rock Obed	28.2	12.8	15.1
Source Rock Obed	4.71	3.85	0.425
Source Rock Obed	1.50	0.584	0.212
Source Rock Obed	3.34	2.46	1.17
Source Rock Sundance	43.0	17.6	30.6
Source Rock Sundance	45.2	37.9	29.1
Source Rock Sundance	60.6	22.7	45.4
Source Rock Sundance	21.7	30.3	14.7
Source Rock Gething	43.2	15.4	32.9
Source Rock Notikewin	13.5	15.4	6.16
Average source rocks:	***27.6***	***15.9***	***18.6***
Cadomin Formation	6.13	4.22	4.25
Cadomin Formation	4.25	3.54	3.08
Blue sky Formation	5.08	2.72	4.78
Blue sky Formation	6.51	3.21	6.26
Average reservoir rocks:	***5.49***	***3.42***	***4.59***

Table 2 : Noble Gas composition for gas samples from sampled gas wells

Sample	^{4}He x10^{-6} (ccSTP/cc)	1σ	R/Ra	1σ	^{36}Ar x10^{-8} (ccSTP/cc)	1σ	$^{40}Ar/^{36}Ar$	1σ	$^{40}Ar^{*}$ x10^{-8} (ccSTP/cc)	1σ	^{84}Kr x 10^{-9} (ccSTP/cc)	1σ	^{136}Xe x 10^{-10} (ccSTP/cc)	1σ
1	20.10	0.016	0.0195	0.0005	3.49	0.03	666	14.3	1281.49	30.11	5.54	0.13	0.53	0.07
2	5.52	0.024	0.0437	0.0008	159.75	1.51	307	4.71	1341.90	24.19	44.22	0.23	7.56	0.21
3					3.67	0.03	301	1.06	8.81	0.09	9.67	0.05	1.62	0.03
4					2.80	0.03	388	43	250.27	27.83	2.06	0.03	0.97	0.03
5	4.12	0.010	0.0725	0.0014	700.00	6.63	296	0.2	0.00	0.00	140.40	0.57	15.23	0.22
6	6.04	0.015	0.0205	0.0007	149.31	1.41	306	1.2	1104.87	11.31	51.19	0.35	9.41	0.22
7	10.79	0.026	0.0246	0.0006	3.13	0.03	517	10.9	684.54	15.78	1.30	0.08	0.42	0.03
8	17.13	0.013	0.0676	0.0006	89.77	0.85	310	0.65	1023.36	9.90	46.21	0.17	16.02	0.26
10	6.56	0.016	0.0195	0.0006	1.09	0.01	630	15.4	361.88	9.40	0.63	0.01	0.23	0.02
11	4.59	0.011	0.0238	0.0008	0.48	0.01	804	22.7	244.27	7.35	0.33	0.01	0.14	0.02
12	6.75	0.017	0.0237	0.0006	2.16	0.02	331	55.9	70.05	11.85	0.55	0.03	0.18	0.04
13	6.07	0.015	0.0312	0.0007	1.29	0.01	411	13	144.50	4.77	0.41	0.50	0.13	0.00
14	5.58	0.021	0.0209	0.0011	2.08	0.02	328	40	61.22	7.49	0.53	0.01	0.14	0.01
16	6.97	0.017	0.0364	0.0013	508.20	4.81	299	0.24	203.28	1.93	115.53	0.45	14.83	0.20
17	5.59	0.014	0.0107	0.0004	0.49	0.00	951	54.3	320.90	18.53	0.31	0.02	0.10	0.02
18	5.01	0.013	0.0152	0.0005	36.46	0.34	295	2.46	0.00	0.00	7.30	0.05	0.86	0.03
19	4.70	0.012	0.0118	0.0009	0.67	0.01	337	34.7	25.76	2.66	0.19	0.01	0.07	0.01
20	5.45	0.014	0.0139	0.0008	1.11	0.01	361	38.6	69.46	7.46	0.33	0.02	0.11	0.01
AIR	***5.20E-07***		***1.00E+00***		***3.12E-05***		***298.6***				***6.50E-07***		***7.71E-09***	
ASW					***1.20E-06***						***4.82E-08***		***1.09E-09***	

Figure captions

Figure 1: Schematic cross sections showing the main differences between a classical field and a basin centered field in terms of pressures and fluid column organisation.

Figure 2: SE-NW cross section of Alberta, modified from Masters, 1979. This geological section is equivalent to the sampling area. Up to eight stacked reservoirs are present in the same well.

Figure 3: Geographic location of sampled wells. The apparent NW-SE alignment of wells is representative of the geological steepening of layers within the basin. Different signs and colors are used to represent each well. They will be fully explained through the discussion part.

Figure 4: Upper panel: Kr versus Xe contents in ccSTP/cc. ASW stands for Air Saturated Water (Porcelli et al., 2002). Air composition is taken also from Porcelli et al. (2002). The compositions of well gas plot on a single mixing line between ASW and an initial signature with a low content in non radiogenic gases (i.e. ^{20}Ne, ^{36}Ar, ^{3}He, Kr and Xe). Lower panel: He content in ccSTP/cc vs. $^{3}He/^{4}He$ ratio. ^{4}He content is high in the gas samples, higher than He content in the air. Combined with Figure 4, upper part, the gas signature appears to be almost only radiogenic.

Figure 5: ^{36}Ar versus depth. As depth increases from NE to SW, this diagram represents the geographical variation of ^{36}Ar from the low pressurized shallow part of the basin (NE) to the high pressurized deeper part (SW). There is a clear trend from the shallow part with a high ^{36}Ar to the deeper part with a low ^{36}Ar, except for 4 wells in the deeper part which have high ^{36}Ar content (see text for explanation).

Figure 6: Conceptual time evolution (from A to D) of $^{136}Xe/^{36}Ar$ versus $^{84}Kr/^{36}Ar$ on the left part and corresponding map of phases interaction. This conceptual model represents a water distillation process seen from the interacted gas composition evolution in the 3 isotope diagram. The gas composition registers not only an interaction with water, but also the intensity of water previous exchanges with former gas generations. G_x stands for gas phase and W_x stands for water phase after x phases interactions. G_0 and W are the initial phases composition before any interaction. G_n and W_n are phases composition after the Nth interaction. It represents the effect of distillation due to repeated interaction between gas and water. If water is in contact with the gas, most of noble gases will be partitioned into the gas phase, as noble gases are more soluble in the gas phase than in water, and the effect increases with the decrease of noble gas mass (light noble gases partition preferentially into the gas phase). If the same batch of water, which is already depleted in noble gases, interacts again with a new batch of gas, the gas phase will not become enriched in ^{36}Ar, but will be slightly enriched in heavy noble gases (Kr, Xe) compared to ^{36}Ar as heavy noble gas will be more soluble in the water phase compared to the light ones.

Figure 7: Left panel: $^{84}Kr/^{36}Ar$ versus $^{136}Xe/^{36}Ar$ diagram showing the evolution of different gas samples interacting repeatedly with the same amount of water as modelized in Figure 6. The gas becomes enriched through the “distillation” of water in heavy noble gases (Kr and Xe) which are more soluble in the water phase than Ar. Black dots, squares and triangles represent samples with a high ^{36}Ar (G_1, Figure 6). Grey dots and squares represent samples which were in contact with “distilled” water (no clear excess in ^{36}Ar but slight enrichment in Kr and Xe, G_2 to G_n, Figure 6). Open dots and squares stand for samples without any influence

of water (G_0, Figure 6). Right panel: Map of the sampling area. The results from the left panel were reported on the map to see the geographical position of water influence.

Figure 8: Left panel: ^{4}He versus $^{40}Ar^{*}$ contents in ccSTP/cc. ^{4}He are considered to be only radiogenic and $^{40}Ar^{*}$ was calculated based on $^{36}Ar/^{40}Ar$ ratio compared to the atmospheric composition. These two radiogenic isotopes were mostly present in the source rock and were a part of the initial signature defined in section 6). Variations in He/Ar ratio provide information on what happened to the gas before any contact with water. The three types of samples defined in comparison with the estimated initial production ratio (relative to the slopes of source rock and reservoir rock) represent an advective transport (Darcy flow - open squares), a diffusive transport (open circles) or a leakage of the reservoir (open triangles). right panel: Map of the sampling area. The results established based on the type of transport (left panel) are reported on the map.

Figure 9: Schematic diagram showing the evolution of ^{4}He contents measured in gas from reservoir layers. Stage 1: before gas generation, ^{4}He is produced mainly in the source rock (S) during diagenesis. Stage 2: first gas generation, most of the ^{4}He produced is removed from the source rock and transferred into the reservoir layer (R), some ^{4}He is taken up during the pathway from some rocks similar in terms of composition to reservoir rocks. Stage 3: continuous gas generation, gas produced in the source rock still migrates to the reservoir layer with a much lower ^{4}He content corresponding to the rate of gas migration. Gas in the reservoir is pushed by the following generations through the porous reservoirs previously filled by water. Stage 4: Mixing in the reservoir. As there is not a large difference (only a factor of 2) of ^{4}He content between the border and the central part of the basin, there must be a mixing of ^{4}He in the reservoir layer, at least a partial mixture.

Figure 10: Map summarizing all the results obtained in this study, integrated in a modelized view of the basin.

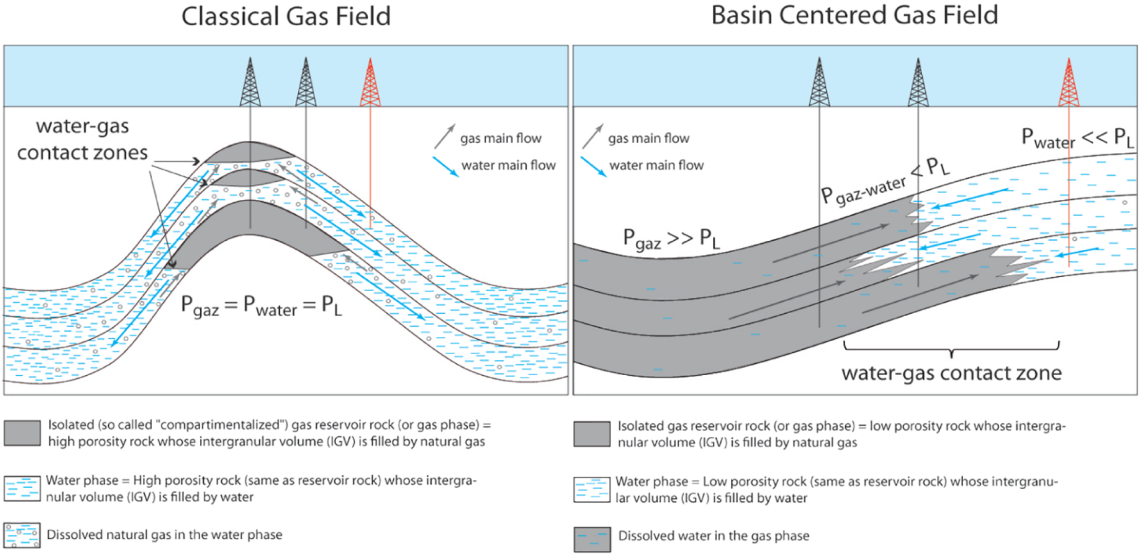
Classical Gas Field
Basin Centered Gas Field
water-gas
contact zones
gas main flow
water main flow
$P_{gaz} = P_{water} = P_L$
gas main flow
water main flow
$P_{water} << P_L$
$P_{gaz-water} < P_L$
$P_{gaz} >> P_L$
water-gas contact zone
Isolated (so called "compartimentalized") gas reservoir rock (or gas phase) = high porosity rock whose intergranular volume (IGV) is filled by natural gas
Water phase = High porosity rock (same as reservoir rock) whose intergranular volume (IGV) is filled by water
Dissolved natural gas in the water phase
Isolated gas reservoir rock (or gas phase) = low porosity rock whose intergranular volume (IGV) is filled by natural gas
Water phase = Low porosity rock (same as reservoir rock) whose intergranular volume (IGV) is filled by water
Dissolved water in the gas phase

Figure 1

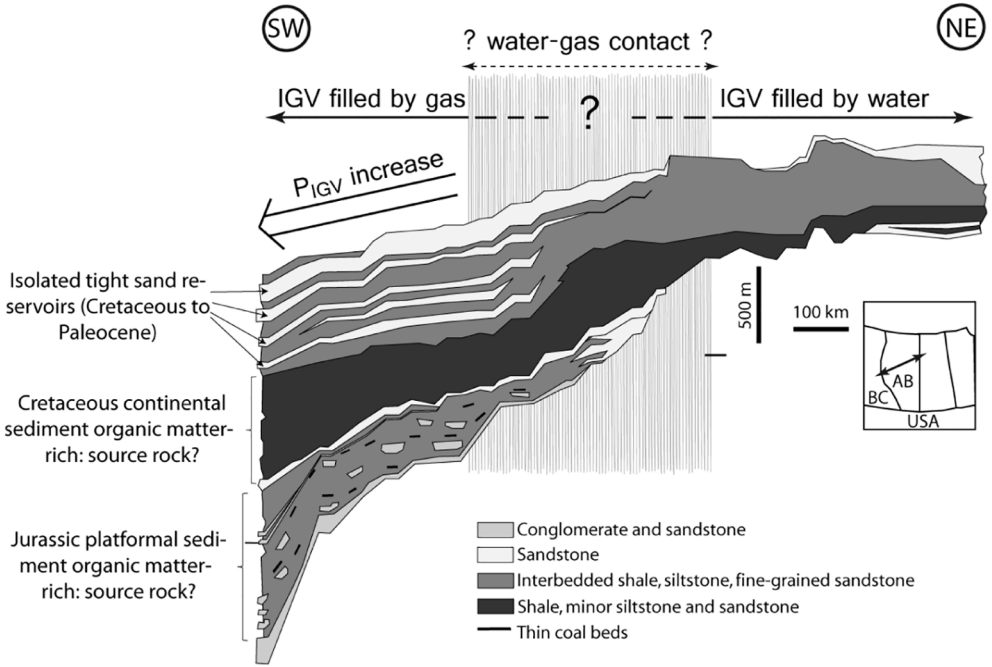
SW
NE
? water-gas contact ?
IGV filled by gas
?
IGV filled by water
P IGV increase
Isolated tight sand reservoirs (Cretaceous to Paleocene)
Cretaceous continental sediment organic matter-rich: source rock?
Jurassic platformal sediment organic matter-rich: source rock?
500 m
100 km
AB
BC
USA
Conglomerate and sandstone
Sandstone
Interbedded shale, siltstone, fine-grained sandstone
Shale, minor siltstone and sandstone
Thin coal beds

Figure 2

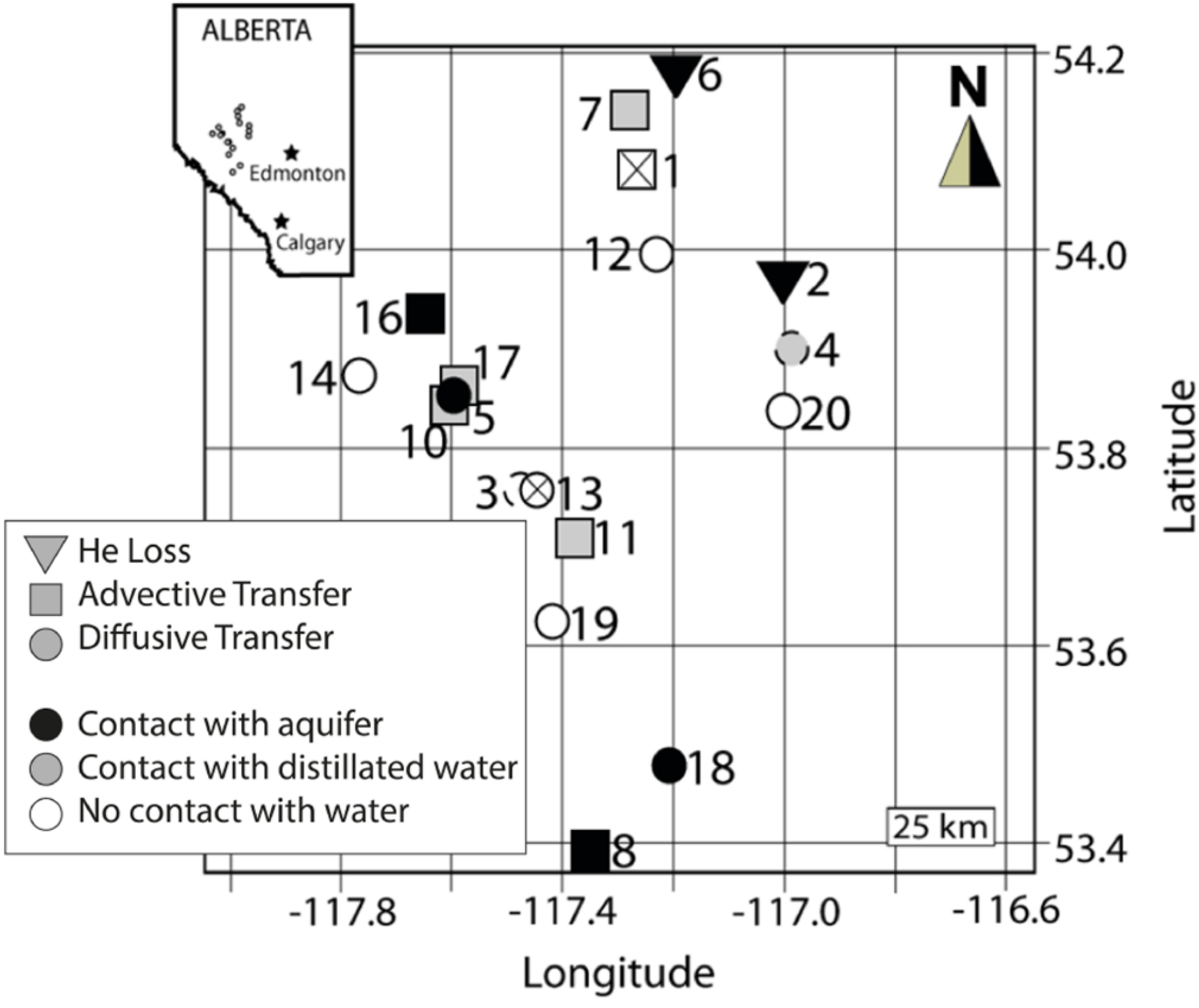
ALBERTA
Edmonton
Calgary
N
25 km
He Loss
Advective Transfer
Diffusive Transfer
Contact with aquifer
Contact with distillated water
No contact with water
1
2
3
4
5
6
7
8
10
11
12
13
14
16
17
18
19
20
54.2
54.0
53.8
53.6
53.4
Latitude
-117.8
-117.4
-117.0
-116.6
Longitude

Figure 3

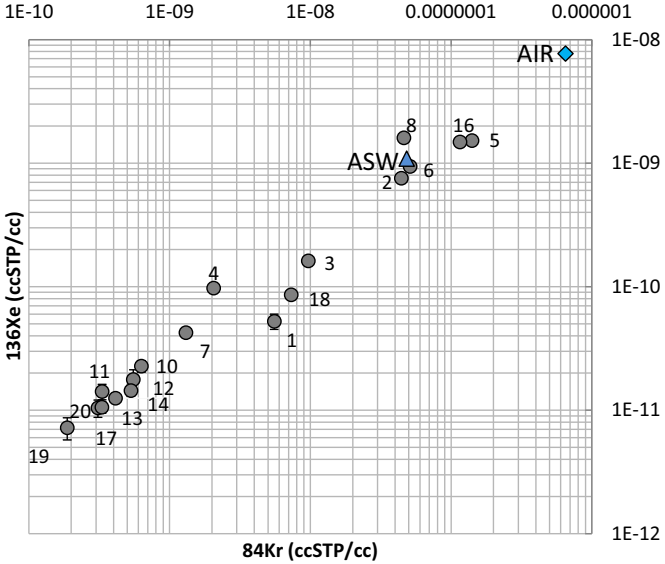
1E-10
1E-09
1E-08
0.0000001
0.000001
1E-08
1E-09
1E-10
1E-11
1E-12
AIR
ASW
136Xe (ccSTP/cc)
84Kr (ccSTP/cc)
1
2
3
4
5
6
7
8
10
11
12
13
14
16
17
18
19
20

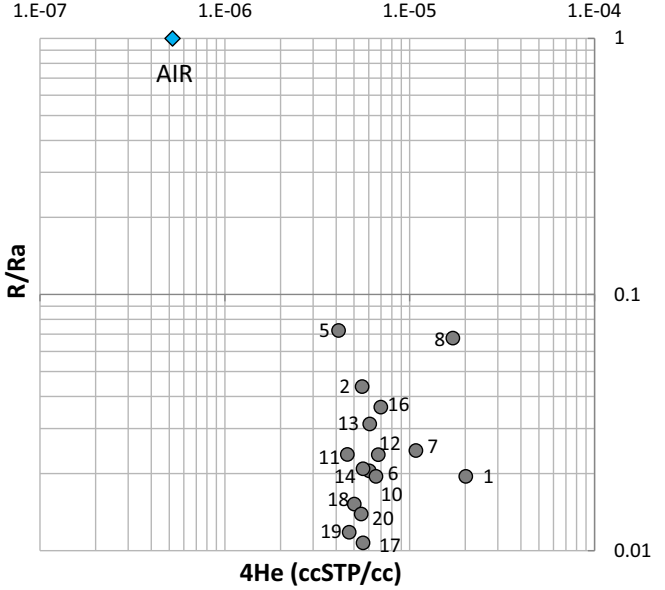
1.E-07
1.E-06
1.E-05
1.E-04
1
0.1
0.01
AIR
R/Ra
4He (ccSTP/cc)
1
2
5
6
7
8
10
11
12
13
14
16
17
18
19
20

Figure 4

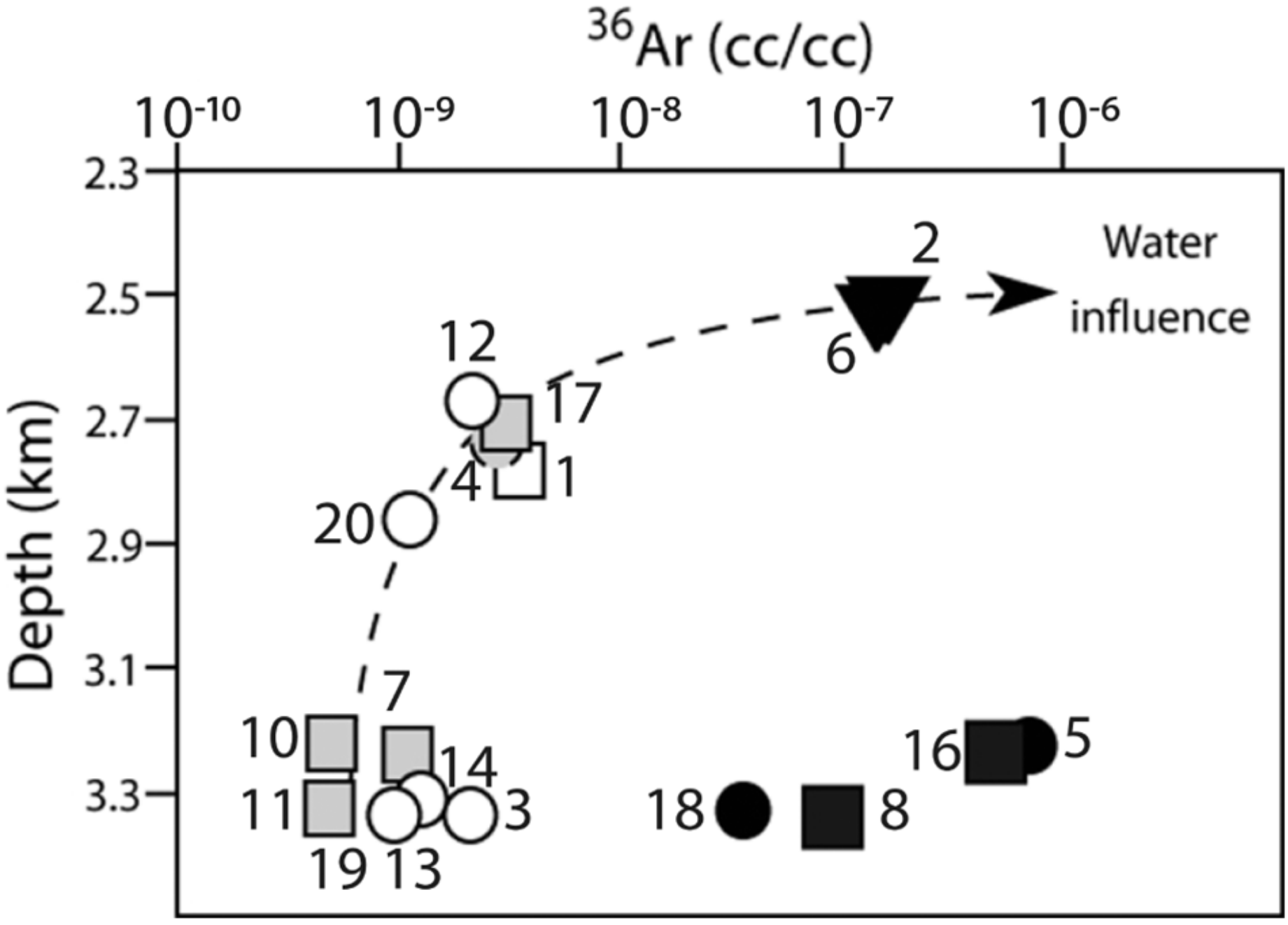
^{36}Ar (cc/cc)
10-10
10-9
10-8
10-7
10-6
Depth (km)
2.3
2.5
2.7
2.9
3.1
3.3
2
Water
influence
6
12
17
4
1
20
7
10
14
11
3
19
13
18
8
16
5

Figure 5

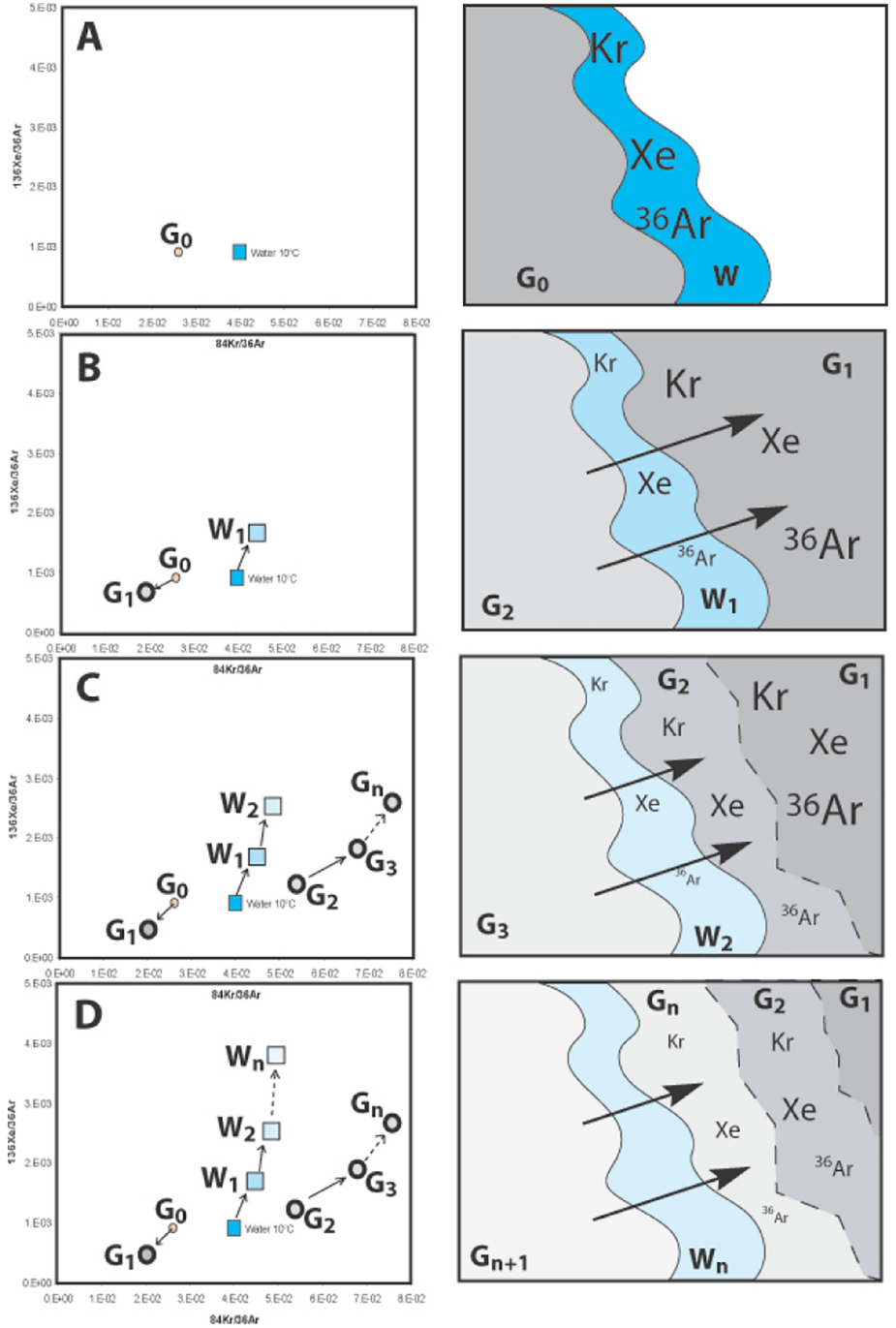
A
B
C
D
136Xe/36Ar
84Kr/36Ar
G0
G1
W1
W2
Wn
Gn
G2
G3
Water 10°C
Kr
Xe
36Ar
W
Gn+1

Figure 6

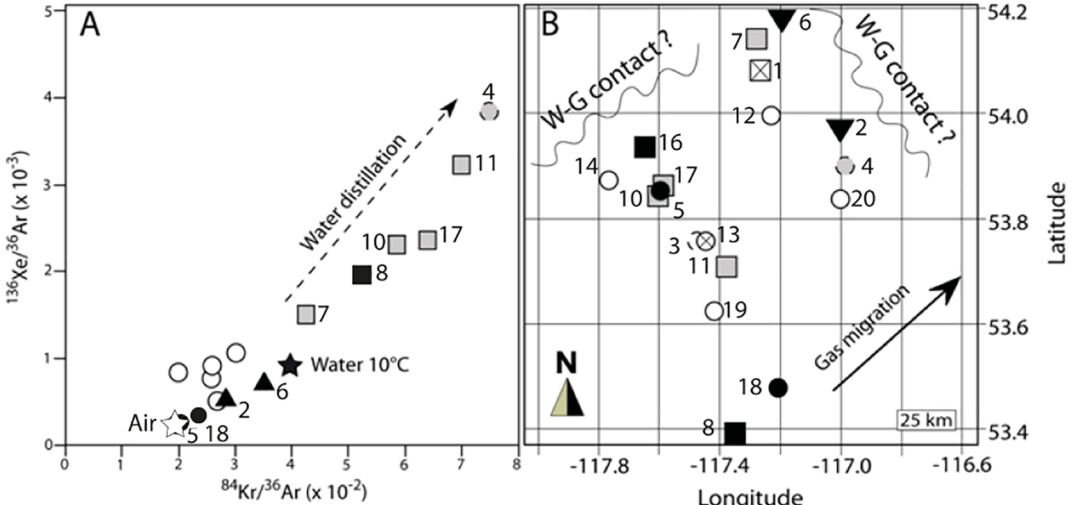
A
B
Water distillation
Water 10°C
Air
W-G contact ?
W-G contact ?
Gas migration
N
25 km
$^{136}Xe/^{36}Ar$ (x 10^{-3})
$^{84}Kr/^{36}Ar$ (x 10^{-2})
Latitude
Longitude
-117.8
-117.4
-117.0
-116.6
54.2
54.0
53.8
53.6
53.4

Figure 7

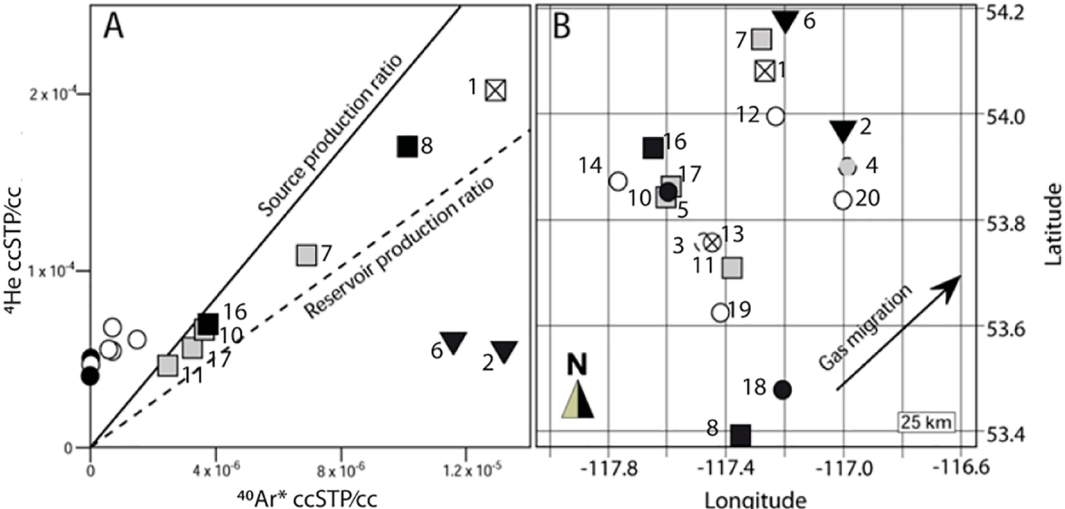
A
B
Source production ratio
Reservoir production ratio
^{4}He ccSTP/cc
^{40}Ar* ccSTP/cc
2 x 10^{-4}
1 x 10^{-4}
0
4 x 10^{-6}
8 x 10^{-6}
1.2 x 10^{-5}
1
2
6
7
8
10
11
16
17
Gas migration
N
25 km
Latitude
Longitude
54.2
54.0
53.8
53.6
53.4
-117.8
-117.4
-117.0
-116.6

Figure 8

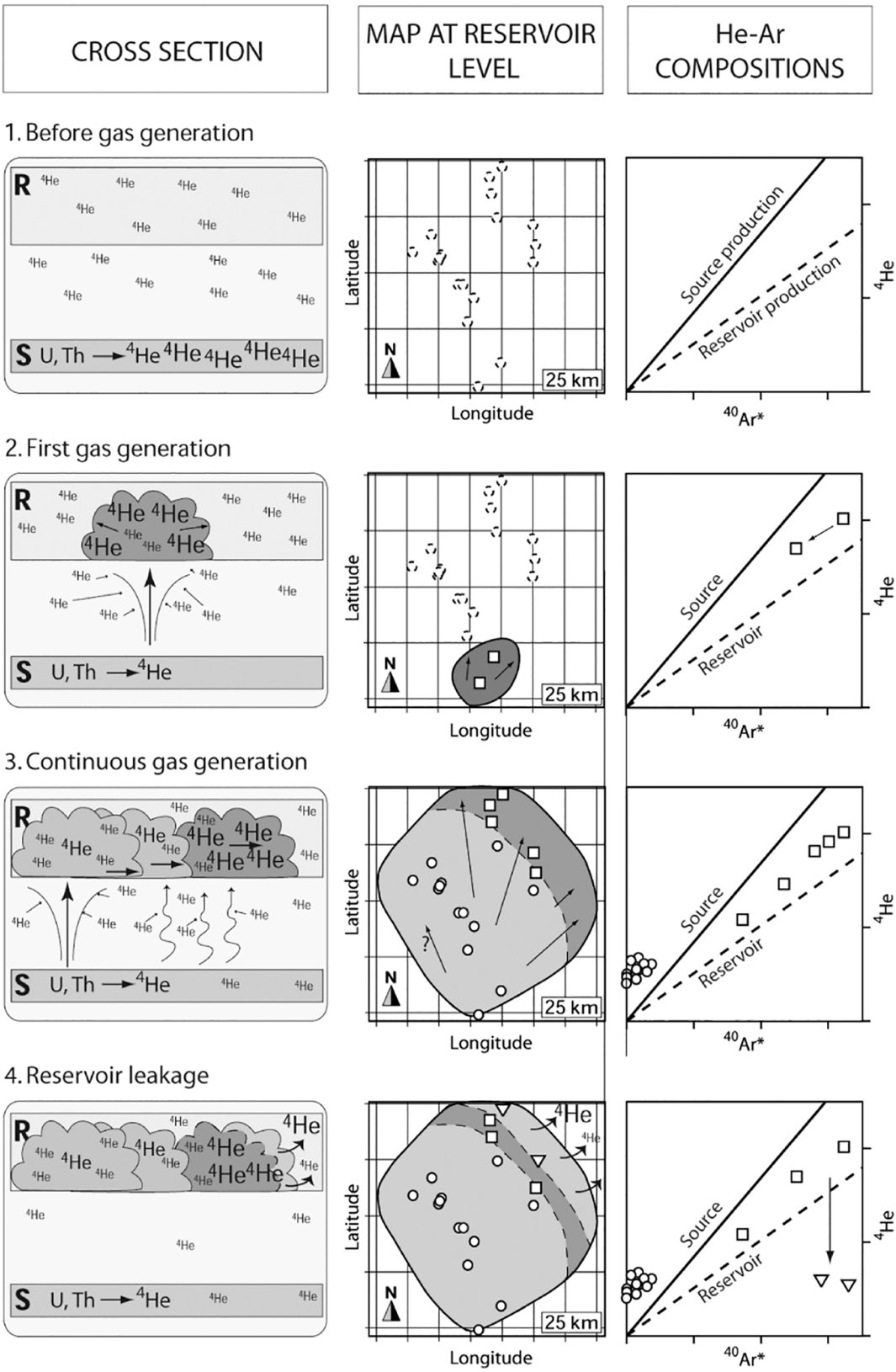
CROSS SECTION
MAP AT RESERVOIR LEVEL
He-Ar COMPOSITIONS
1. Before gas generation
R
S U, Th → 4He 4He 4He 4He 4He
Latitude
Longitude
N
25 km
Source production
Reservoir production
4He
40Ar*
2. First gas generation
S U, Th → 4He
Source
Reservoir
3. Continuous gas generation
?
4. Reservoir leakage

Figure 9

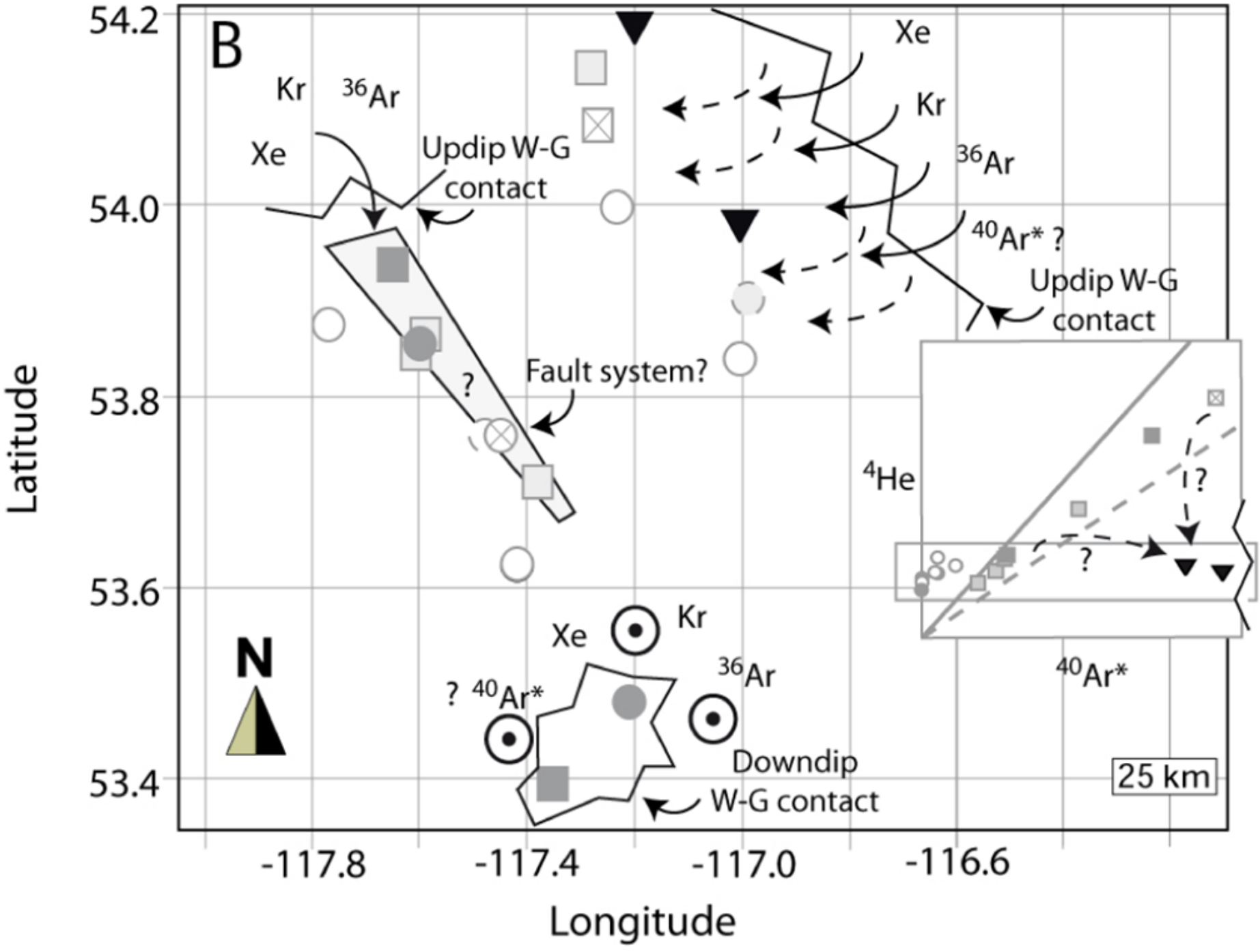
B
Kr
36Ar
Xe
Updip W-G
contact
Xe
Kr
36Ar
40Ar* ?
Updip W-G
contact
Fault system?
?
4He
?
?
40Ar*
Xe
Kr
36Ar
? 40Ar*
Downdip
W-G contact
N
25 km
54.2
54.0
53.8
53.6
53.4
-117.8
-117.4
-117.0
-116.6
Latitude
Longitude

Figure 10